Receptor-mediated endocytosis of lysozyme in renal proximal tubules of the frog *Rana temporaria*

E.V. Seliverstova, N.P. Prutskova

Sechenov Institute of Evolutionary Physiology and Biochemistry of the Russian Academy of Sciences, St. Petersburg, Russia

Abstract

The mechanism of protein reabsorption in the kidney of lower vertebrates remains insufficiently investigated in spite of raising interest to the amphibian and fish kidneys as a useful model for physiological and pathophysiological examinations. In the present study, we examined the renal tubular uptake and the internalization rote of lysozyme after its intravenous injection in the wintering frog *Rana temporaria* using immunohisto- and immunocytochemistry and specific markers for some endocytic compartments. The distinct expression of megalin and cubilin in the proximal tubule cells of lysozyme-injected frogs was revealed whereas kidney tissue of control animals showed no positive immunoreactivity. Lysozyme was detected in the apical endocytic compartment of the tubular cells and colocalized with clathrin 10 min after injection. After 20 min, lysozyme was located in the subapical compartment negative to clathrin (endosomes), and intracellular trafficking of lysozyme was coincided with the distribution of megalin and cubilin. However, internalized protein was retained in the endosomes and did not reach lysosomes within 30 min after treatment that may indicate the inhibition of intracellular trafficking in hibernating frogs. For the first time, we provided the evidence that lysozyme is filtered through the glomeruli and absorbed by receptor-mediated clathrin-dependent endocytosis in the frog proximal tubule cells. Thus, the protein uptake in the amphibian mesonephros is mediated by megalin and cubilin that confirms a critical role of endocytic receptors in the renal reabsorption of proteins in amphibians as in mammals.

Introduction

Within the last few years, the kidney of aquatic and terrestrial amphibians serves as a useful experimental system for investigating the molecular mechanisms of various physiological processes. They include the filtration-reabsorption processes,[1-3] different transport systems,[1,4] and some renal pathological alterations.[5-7] The unique anatomy of the urodelic amphibian kidney including open nephrons connected with peritoneal funnels (nephrostomes) makes it possible to investigate the tubular uptake of protein and non-protein nephrotoxic substances injected into the peritoneal cavity, without glomerular filtration. Such investigation of the process of tubulointerstitial activation and induction of interstitial fibrosis by protein loading was performed on the axolotl kidney.[5,6] This takes on special significance of amphibian kidney for studying the renal tubular disorders similar to human kidney disease induced by protein overloading and/or endocytic receptor dysfunction.[8] Novel data about the protein absorption under conditions of hydration and by antidiuretic hormone treatment in the anuran amphibian *Rana temporaria* were obtained in our previous works.[9-12] In spite of some morphological peculiarities of the amphibian nephrons[13-15] it was shown the amphibian kidneys, embryonic and adult, function by the same filtration-reabsorption processes as mammalian kidneys.[1,2] The use of the frog kidney as an experimental model requires the strong knowledge of mechanisms involving in tubular reabsorption of various macromolecules, but the information about this process in non-mammals is still insufficient. The renal uptake studies in mammals provide much evidence that the proximal tubule cells absorb the proteins from the tubular fluid by means of receptor-mediated endocytosis, and then absorbed proteins are transported into endosomes and lysosomes for the subsequent degradation.[16-18] According to the latest conceptions, this process involves two interacting receptors, megalin and cubilin, which form a complex with amnionless.[17-20] The cubilin-amnionless complex mediated internalization of proteins, and megalin performs internalization of cubilin-protein complex.[18,20] Megalin and cubilin are expressed in the apical pole of renal proximal tubule cells. At the subcellular level they are revealed in the early endocytic compartment (apical clathrin coated pits, vesicles and early endosomes). Both receptors are also detected in the apical recycling compartment, dense apical tubules. Expression of these receptors in the late endosomal compartment and lysosomes appears more limited.[17]

In lower vertebrates, as opposed to mammals, the evidences of megalin-cubilin-dependent endocytosis are not numerous. According to the study in the *Xenopus pronephric* kidney,[17] the expression of endocytic receptors (megalin/LRP2, cubilin, and amnionless) in proximal tubule and the availability of protein endocytosis were established. In our previous study, the involving cubilin and megalin in the uptake and vesicular transport of yellow fluorescent protein (YFP) in the proximal tubule cells of the *R. temporaria* kidney was shown.[12] As regards other lower vertebrates, similar data on megalin- and cubilin-dependent endocytosis were obtained only for the zebrafish pronephros.[21] The endocytic uptake and intracellular accumulation in the mammalian proximal tubules were first described for larger proteins (albumin, hemoglobin, horseradish peroxidase), but later it was shown that small proteins such as growth hormone, lysozyme, and insulin are absorbed by the same way.[22-24] Lysozyme is known as a protein extensively filtering and completely absorbing by the tubular epithelium.[23-26] It allows to actively using lysozyme as a carrier for renal-specific delivery of various drugs in the drug-targeting technologies.[27,28] In mammals, intracellular trafficking of lysozyme is completely investigated,[22,23,25,29,30] and lysozyme is regarded as a specific ligand of low density lipoprotein receptor family members.[16,17] Nevertheless there are few studies about the direct involvement of megalin and cubilin in the internalization of lysozyme by the proximal tubule cells in mice and rats.[28,30]

Based on our previous frog studies which have demonstrated the tubular reabsorption and uptake pattern of model proteins, green fluorescent protein (GFP) and YFP,[11,12] it was reasonable to examine the mechanisms of endocytosis in the frog kidney using different proteins, in particular, lysozyme. Taking into account the detailed data about this filterable low molecular weight protein including the mechanisms of its tubular reab-

Correspondence: Elena V. Seliverstova, Sechenov Institute of Evolutionary Physiology and Biochemistry of the Russian Academy of Sciences, Laboratory of Renal Physiology, Torez Av., 44, 194223 St. Petersburg, Russia.
Tel. /Fax: +7.812.5523086.
E-mail: elena306@yandex.ru

Key words: Endocytic receptor, frog, kidney, lysozyme, protein uptake, proximal tubule.

Funding: the reported study was supported by the Russian Foundation for Basic Research, project No. 13-04-00039.

Received for publication: 9 January 2015.
Accepted for publication: 24 February 2015.

European Journal of Histochemistry 2015; 59:2482
doi:10.4081/ejh.2015.2482

sorption in mammals, the expected results could be very informative for comparative physiological analysis of receptor-mediated endocytosis in vertebrates. It also may be useful for further employment of this system for investigation of renal tubular disorders. The aim of the present study was to identify the tubular uptake and internalization route of lysozyme in the *R. temporaria* kidney after its intravenous injection using immunochemistry, immuno-electron and confocal microscopy and employing specific markers for some intracellular compartments.

Material and methods

Animals

Experiments were carried out on wintering male frogs (*R. temporaria*) from November to April. Animals (38±1 g BW, n=38) were housed in plastic tanks with tap water at 4ºC and were kept in individual tanks for one hour at room temperature (RT) before the experimental procedure. The depth of water was sufficient to ensure complete hydration of frogs. The protocol of all experiments was approved by the Bioethics Committee of the Institute (Protocol 4 of 17.01.2013).

Experimental protocol

Immobilized (double-pithed) frogs were placed on a Petri dish containing tap water sufficient to immerse the frog's pads and ventral pelvic skin during the experiment. Chicken egg white lysozyme was diluted in 0.01 M phosphate-buffered saline (PBS) with 111 mM NaCl, pH 7.4, osmolality 230 mOsm/kg H_2O. The lysozyme was injected into a peroneal vein at a dose 18 µg/100 µL/30 g BW. Control animals were non-injected or injected with PBS. At 10, 20 and 30 min after injection the kidneys were removed, replaced into fixative solutions, dissected and treated for further investigation.

Fixation and tissue treatment

For immunofluorescence tissue blocks were fixed by immersion in 4% PFA/PBS solution (230 mOsm) for 3-4 h at 4ºC , rinsed with PBS and cryoprotected in 30% sucrose/PBS overnight. Then samples were transferred to Tissue-Tek® OCT (Sakura, Torrance, CA, USA) and frozen in liquid nitrogen. Cryostat sections (5-7 µm) were cut using a Leica cryostat CM 1510 (Leica Microsystems, Wetzlar, Germany) at -20ºC, mounted onto polylysine covered microscope slides (Menzel-Gläser, Braunschweig, Germany), and air-dried at RT. For immunocytochemical studies small pieces of the tissue were fixed in 0.5% glutaraldehyde (Sigma-Aldrich, St. Louis, MO, USA) mixed with 4% paraformaldehyde (Sigma-Aldrich) in 0.01 M PBS, pH 7.3 overnight at 4ºC. After washing with PBS (2×10 min) specimens were dehydrated in ethanol series at 4 C, infiltrated by cold LR White resin (Agar Scientific Ltd., Stansted, UK) transferred into resin-filled gelatin capsules, and underwent polymerization using a UV-chamber (Agar Scientific Ltd.). Ultrathin sections (50-70 nm) were cut with Leica Ultracut UCT (Leica Microsystems) and placed on butvar-coated nickel grids.

Immunohistochemical analysis

Cryostat sections were pre-incubated with PBS for 30 min and permeabilized with PBST (0.2% Triton X-100 in 0.01M PBS) for 30 min. After blocking with nonfat 5% dry milk in PBST for 1 h, sections were washed in PBST for 1 min, blocked in 5% BSA in PBTS for 1 h, washed two times in PBST for 5 min and incubated with primary antibody in 1% BSA-PBST overnight at 4ºC. The following dilutions were used for immunohistochemistry: polyclonal rabbit anti-human megalin or cubilin diluted 1:25, rabbit anti-hen lysozyme (1:100), monoclonal mouse clathrin (1:50), mouse anti-rat caveolin-1 (1:50), mouse anti-human LAMP1 (1:50). The primary antibodies were omitted from the incubation solution as negative control. Next day sections were washed six times in PBST for 5 min and incubated with secondary goat anti-rabbit IgG conjugated with Alexa Fluor 488 (1:500) and donkey anti-mouse IgG conjugated with Alexa Fluor 568 (1:500) respectively in the same incubation medium for 1 h at RT. After six washes in PBST for 5 min, sections were washed six times in PBS for 5 min, washed once in H_2O, and then covered with a glass coverslip using Fluorogel (Electron Microscopy Science, Hatfield, PA, USA). Samples were examined with a confocal Leica TCS SP5 inverted microscope (Leica Microsystems, Inc., Bannockburn, IL, USA) equipped with an argon and helium-neon lasers. Alexa Fluore 488 was visualized with excitation and emission wavelengths of 488 nm and 515 nm, respectively. The corresponding wavelengths for Alexa Fluor 568 were 543 nm and 605 nm. Images were obtained using a colour digital camera Leica DFC300 FX.

Immunocytochemical analysis

Electron microscope immunocytochemistry was performed using post-embedding immunogold technique. Ultrathin sections were incubated with 0.01M PBS, followed by incubation with 0.05 M glycine, pH 7.4 for 30 min at RT. For background elimination the sections were blocked with 1% BSA-PBS for 1 h and incubated with primary antibody diluted in 0.1% BSA-PBS overnight at 4ºC in a humidified chamber. For EM labeling the following antibodies were used: polyclonal rabbit anti-human megalin or cubilin diluted 1:10, rabbit anti-hen lysozyme (1:60, 1:100), monoclonal mouse anti-clathrin (1:500). The primary antibodies were omitted from the incubation solution as negative control. After overnight incubation sections were rinsed six time for 10 min with PBST (0.01M PBS with 0.1% BSA and 0.02% Tween® 20) and then incubated with secondary antibody p-A-Gold conjugate (10-15 nm) diluted 1:50 in 0.1% BSA-PBS for labeling of primary polyclonal antibody for 1 h at RT. For labeling of mouse monoclonal primary antibody we used intermediate treatment with bridging rabbit anti-mouse IgG diluted 1:50 for 30 min at RT followed by incubation with p-A-Gold in the same incubation medium. After six washes with PBST and additional two washes with PBS sections was fixed with 1% glutaralgehyde, washed with distilled water and dried. Ultrathin sections were doubly stained with uranyl acetate and lead citrate and examined in a Tecnai G2 Spirit transmission electron microscope (FEI, Eindhoven, The Netherlands) at 80 kV. Electron micrographs were obtained by Olympus-SIS Mage View G2 CCD Camera, images were transferred (digitally transferred) by TEM Imaging and Analysis Software (TIA program) and processed by using Adobe Photoshop 8.0 (Adobe Systems, Mountain View, CA, USA).

Antibodies and chemicals

Lysozyme from Chicken Egg White was purchased from Sigma (Sigma-Aldrich), p-A-Gold conjugate (15 nm) was purchased from EMS (Electron Microscopy Science). The following antibodies were used: polyclonal rabbit anti-human megalin (H-245) and rabbit anti-human cubilin (H-300) (Santa Cruz Biotechnology Inc., Santa Cruz, CA, USA); rabbit antibody to lysozyme from hen egg white (Abcam Inc., Cambridge, MA, USA); monoclonal mouse antibody to clathrin LC (3F133), mouse anti-rat antibody to caveolin-1 (7C8), and mouse anti-human antibody to LAMP1 (E-5) (Santa Cruz Biotechnology); goat anti-rabbit-Alexa 488 IgG and donkey anti-mouse-568 IgG (Invitrogen, Molecular Probes, Carlsbad, CA, USA); bridging rabbit anti-mouse IgG (Zymed Laboratories, Invitrogen, USA).

Statistical analysis

All data are presented as means±SEM. The average values of fluorescent vesicles (per 5 neighboring cells) in proximal tubule profiles were calculated (3 frogs, 30 tubules for each experiment). The number of proximal tubule profiles with immunolabeled lysozyme was calculated as percentages relative to the total number of profiles (60-120 profiles for each frog) visualized in confocal images of the dorsolateral area of kidney sections. Multiple comparisons were made using one-way ANOVA followed by a Newman-Keuls test. The results were considered to be statistically significant at $P<0.05$.

Results

Lysozyme uptake in the frog proximal tubules

The initial immunohistochemical evaluation of the lysozyme intravenous injection revealed a distinct intracellular labeling in proximal tubule profiles at different time points of the experiment (Figure 1 A-C). The distal tubules and other parts of the nephron showed no positive immunoreactivity (Figure 1 B,C). No specific fluorescence was also detected in kidney tissue of control animals, non-injected or injected with PBS (Figure 1F). There was no staining following the incubation of kidney sections without the primary antibody (*not shown*). Immunofluorescent label in the epithelial cells was mostly intracellular and punctate, suggesting the localization of lysozyme in a vesicular compartment (Figure 1 A-E). Light fluorescence of the brush border was also detected (Figure 1 D,E). The intracellular distribution of lysozyme changed with increase of the time after its introduction. After 10 min, a linear arrangement of lysozyme-containing vesicles was detected close to the brush border (Figure 1 A,D). With increasing time (20 and 30 min), vesicular structures were located deeper in apical cytoplasm, the number of vesicles significantly increased (Table 1), and fluorescence staining was appeared more intensive (Figure 1 B,C,E). The analysis of the lysozyme uptake pattern showed some tubules in the dorsolateral part of the kidney demonstrating the positive fluorescence signal 10 min after injection (Figure 1A; Table 1). After 20 and 30 min, the number of the proximal tubule profiles with internalized lysozyme was increased in comparison with 10 min (Figure 1 B,C; Table 1). It should be noted, that immunofluorescent signal in the early proximal tubule appeared more intensive than in the late segments at the same time points of the experiment (Figure 1 A,C). So, the accumulation and distribution of labeled lysozyme increased in a time-dependent manner and reflected progressive internalization of injected protein (Table 1).

Electron microscopy showed well-preserved ultrastructure of the proximal tubule cells within 30 min after introduction of lysozyme (Figure 2A). The endocytic apparatus, includ-

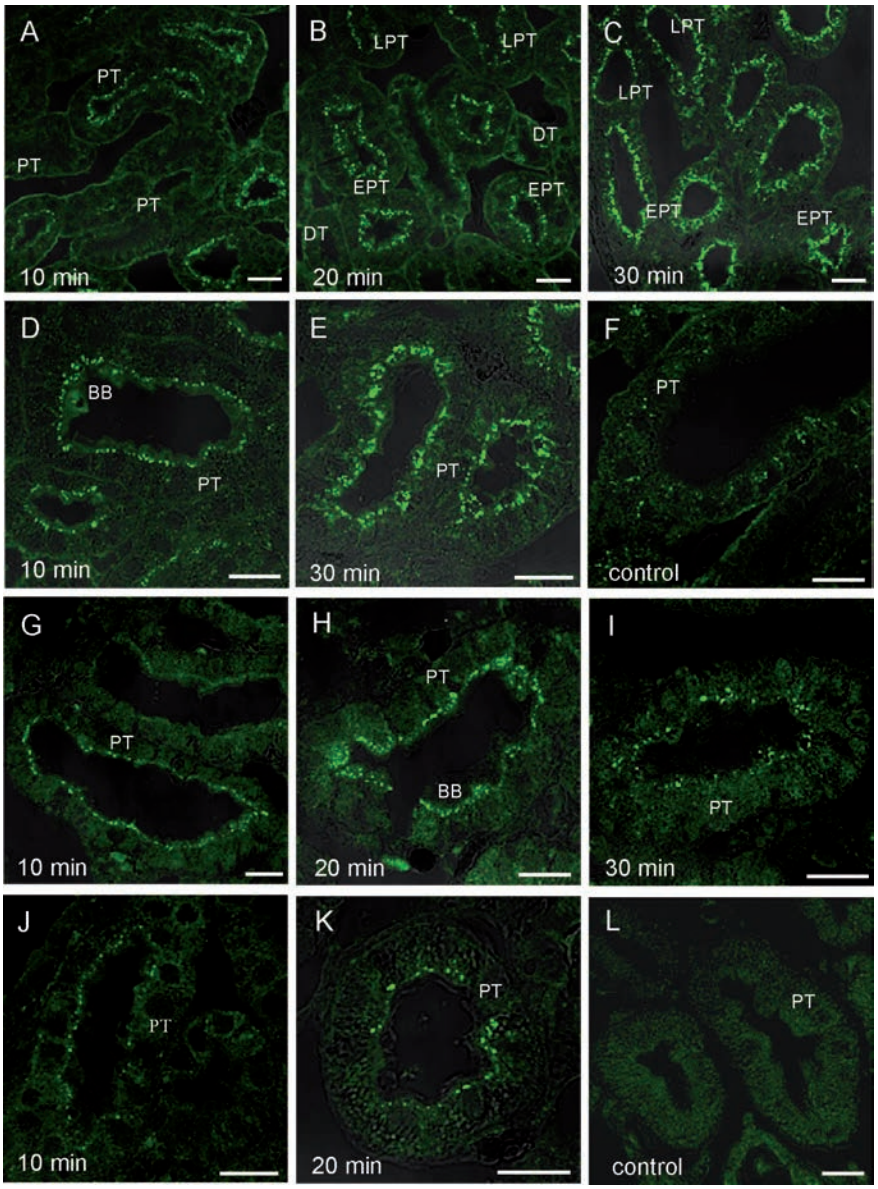

Figure 1. Immunofluorescent detection of lysozyme and endocytic receptors in the frog proximal tubules. A-E) Time-depending localization of lysozyme in the proximal tubule cells demonstrating vesicular accumulation of injected protein; note spreading distribution of labeled protein in the apical area of the epitheliocytes and increasing intensity of fluorescence signal within 30 min after injection. F) Negative stained tubular epithelium in control (PBS-injected) frogs. G-I) Time-dependent megalin expression in the proximal tubule cells from lysozyme-treated frogs; note the initial apical expression of this receptor (G) and its following internalization (H,I). J,K) The same (as in G-I) for cubilin; the intensity of cubilin immunofluorescence is notably reduced compared with megalin. L) Anti-megalin antibody negative staining of the proximal tubules in control (non-injected) animals. Figure presents merged fluorescence and bright-field micrographs. BB, brush border; DT, distal tubule; EPT, early proximal tubule; LPT, late proximal tubule; PT, proximal tubule. Scale bars, 25 μm.

Table 1. Time-dependent uptake of lysozyme in the frog proximal tubules.

Time after lysozyme injection	10 min	20 min	30 min
Number of lysozyme-containing vesicles in epithelial cells	14.2±0.3	20.5±0.3*	28.2±0.4[#]
Number of proximal tubule profiles with internalized lysozyme (%)	34.6±3.6	56.0±3.3[§]	65.8±3.1[§]

Data are expressed as the mean±SEM of 3 experiments. *P<0.001 *vs* 10 min; [#]P<0.001 *vs* 10 and 20 min; [§]P<0.05 *vs* 10 min.

ing vesicles, vacuoles, dense apical tubules, and endosomes appeared intact. Electron immunocytochemistry detected the gold label in the inter-microvillar space, in the cell cytoplasm underneath the brush border including apical invaginations and endocytic vesicles 10 min after lysozyme injection (Figure 2B). Fusion of small and large apical vesicles containing gold particles was observed. The label was distributed over the large vesicles and their membranes (Figure 2C). Such vesicles (diameter up to 1 μm) were filled by amorphous material or were electron-transparent. The staining was partly found in large apical semi-dense vesicles, presumably corresponding to late endosomes and/or lysosomes 30 min after injection (Figure 2D).

Detection of endocytic receptor expression

Immunohistochemistry using antibody against megalin revealed clear labeling of this receptor in the proximal tubules of lysozyme-treated frogs (Figure 1 G,H) whereas no immuno-positive staining was found on kidney sections from control animals (Figure 1L). There was no detectable signal associated with other segment of the nephrons. The fluorescent signal was localized in the apical pole of the proximal tubule cells, and relatively little signal was observed at the brush border. Staining was distributed diffusely along the base of the brush border or was punctate 10 min after lysozyme injection (Figure 1G). At 20 and 30 min after injection, the vesicular fluorescence was predominantly found in the subapical area of the tubule cells and expression of megalin appeared more intensive (Figure 1 H,I). In some proximal tubules, fluorescence seemed to be returned to the apical area of cytoplasm and became again diffuse. The similar distribution was determined for cubilin (Figure 1 J,K), however the expression of megalin was seemed more intense compared with cubilin at all time points of the experiment (Figure 1 G-J).

Immuno-electron microscopy with the same antibody application revealed more detailed localization of both receptors in apical endocytic structures of the epitheliocytes. Cubilin and megalin gold staining was observed in apical membrane invaginations, probably representing coated pits. These receptors were also detected in small endocytic vesicles near the brush border and in apical larger vesicular structures (endosomes) (Figure 2 F,G). Rather little labeling is found in the brush border. Thus, the expression of cubilin and megalin occurred in the similar sites of the frog tubule cells, but expression of megalin was more pronounced.

Immunodetection of clathrin

In order to detect whether the internalization of lysozyme in the frog proximal tubules occurs *via* clathrin-coated vesicles, antibody against clathrin was used. Specific fluorescence signal was revealed in the most proximal tubules of lysozyme-injected frogs, and the other parts of nephron displayed no positive staining (Figure 3 A,B). The expression of clathrin was also found in control animals, but it was significantly decreased compared with lysozyme-treated frogs (Figure 3C). Application of caveolin-1 antibody as a marker of the non-clathrin pathway did not revealed any immunoreactivity in kidney sections from lysozyme-injected and control frogs (*not shown*). Immunofluorescence showed that staining for clathrin was diffusely distributed below the brush border 10 min after injection (Figure 3A). After 20 and 30 min, the distribution of clathrin was similar, but the fluorescence appeared more intensive (Figure 3B), while immuno-staining in control frogs remained former (Figure 3C). Clathrin labeling in the early proximal tubules was more intensive and extended than one in the late segments at all time points after injection. Immuno-gold labeling revealed that clathrin was located in intermicrovillar invagination of the luminal membrane and apical vesicular structures (Figure 2E). Gold particles appeared

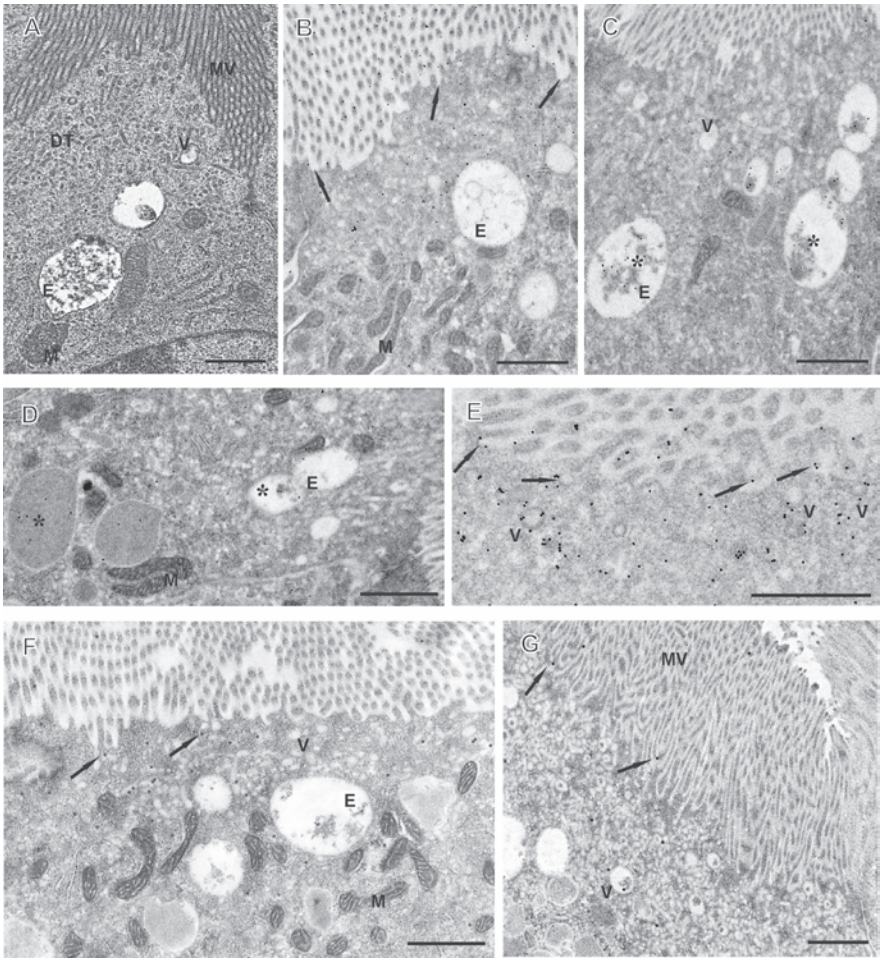

Figure 2. Electron micrographs of the proximal tubule cells from lysozyme-injected frogs. A) Well-preserved ultrastructure of endocytic apparatus epithelial cells after lysozyme injection. B-G) Post-embedding immunogold labeling of ultrathin LR-White sections from the frog kidneys. B-D) Immunogold staining of lysozyme 10 min (B, C) and 30 min (D) after injection; label is detected over the brush border, in apical vesicles, endosomes and vesicles with a semi-dense content (D). E) Localization of clathrin in microvilli and apical vesicles in the tubular cells 10 min after injection. F) Immunolabeling of megalin in the tubular cells of lysozyme-treated frogs 10 min after injection; localization of this receptor in apical endocytic compartment is shown. G) The same for cubilin. Arrow shows the label in apical coated pits; asterisk shows immunogold particles in vesicles. E, endosome; M, mitochondria; MV, microvilli; V, apical vesicle. Scale bars, 1 μm.

to be distributed randomly over the surface of apical vesicles. The clear gradient of labeled clathrin distribution was observed from brush border towards the deeper areas of cytoplasm (Figure 2E).

Double labeling with antibodies against lysozyme and clathrin revealed that injected protein was colocalized with clathrin in the apical endocytic compartment of the tubular cells 10 min after injection (Figure 3 D-F). At the same time, the divergence of labels for clathrin and lysozyme were observed in some proximal tubules (Figure 3G) indicating that lysozyme starts to leave the early endocytic compartment. After 20 and 30 min, no overlapping of labeled lysozyme and clathrin was observed (Figure 3H) that may reflect complete localization of injected protein in the endosomal compartment of the cells.

Lysozyme accumulation

To determine the accumulation of lysozyme in the late endocytic compartment we used antibody against defined lysosomal marker LAMP1. Immunofluorescent microscopy revealed LAMP1-positive vesicular structures in central and basal area of the epithelial cells. Double labeling using lysozyme antibody did not reveal the overlap of injected protein with LAMP1 at all time points of the experiment (Figure 3 I,J). Labeling of lysozyme remained still apical even 30 min after protein injection. These results indicate that lysozyme did not moved into late endosomes and/or lysosomes within 30 min after treatment. Electron microscopy observation showed large semidense vesicles which was distinct from the early endocytic structures in the proximal tubule cells (Figure 2D). Some of these vesicles displayed sparse labeling of lysozyme (Figure 2D), that might be probably a non-specific reaction and the results of more sensitive immunofluorescent method were considered as more convincing (Figure 3 I,J).

Discussion

The present study showed that intravenous injection of lysozyme resulted in the intracellular accumulation of protein in the frog proximal tubules (Figure 1 A-C). Immunofluorescent microscopy analysis revealed that labeled lysozyme was mainly located in apical vesicles within 10 min after introduction with following movement to the subapical area of the cells. The number of vesicles (Table 1) and intensity of fluorescent label was increased within 30 min of the experiment. Thus, the lysozyme internalization was time-dependent as well described in mammals.[22,23,25,29] In rat experiments, tubular absorption of injected lysozyme was rapid for first 10 min,[28,31] and then protein was absorbed gradually[27] and the maximum protein accumulation (under 80% of injected protein amount) was appeared within 30 min.[23,25] In our previous studies, the similar time-course of GFP and YFP accumulation in frog proximal tubule cells was occurred.[9,11,12] Immunoelectron microscopy revealed that injected lysozyme was located in the brush border area and early endocytis compartment, and mainly distributed in larger apical vesicles (Figure 2 B,C). These results are corroborated with previously demonstrated intracellular localization of injected lysozyme in apical vacuoles of the rat proximal tubule cells using electron microscope autoradiography.[22,25] So, the initial stage of lysozyme internalization in the kidney of *R. temporaria* appears similar to this process in mammals.

Although the intracellular pathway of lysozyme is well studied in rats and mice,[22,23,25,29,30,32] the direct involvement of endocytic receptors in lysozyme internalization is insufficiently investigated. A great number of *in vitro* and *in vivo* studies in mammals including megalin and cubilin deficient mice[16,30,33] and dogs with functional cubilin deficiency[16,34] have provided strong evidence that cubilin and megalin are the key receptors for endocytosis of various macromolecules.[17,18] These multiligand receptors are responsible for the endocytic uptake of a large number of different proteins and peptides, including lipoproteins, hormones, nutrients, and enzymes.[16,17] In the present work, immunohisto- and immunocytochemical examination

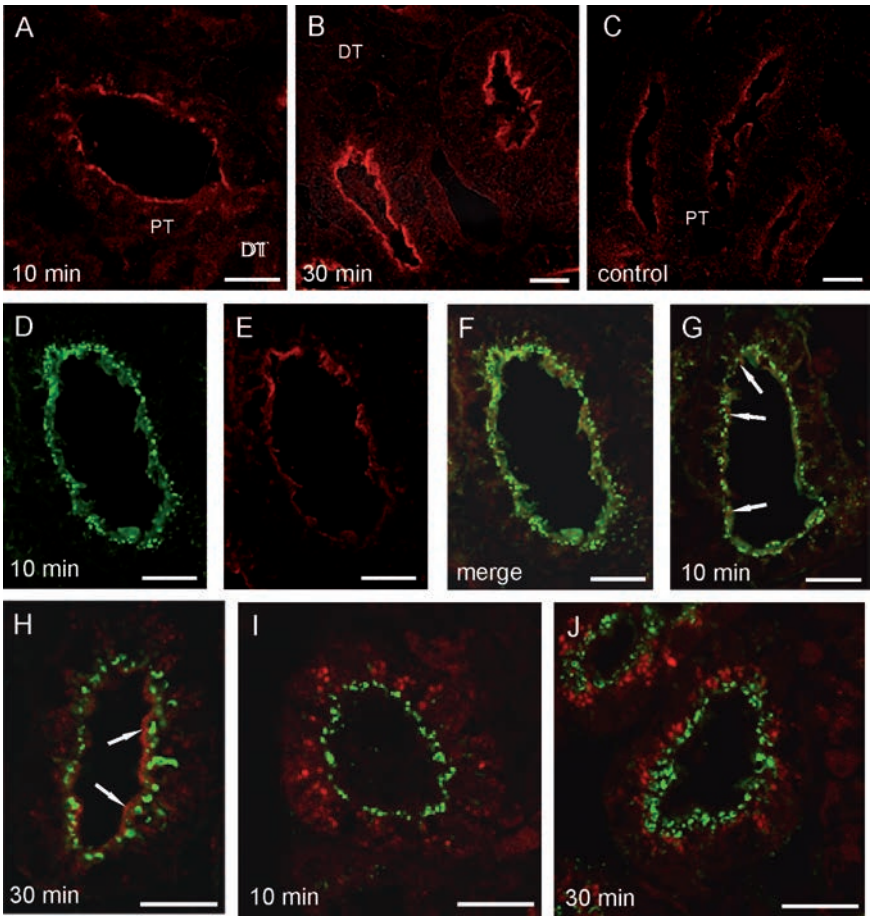

Figure 3. Immunofluorescent detection of lysozyme internalization rote in the frog proximal tubule cells using antibodies against lysozyme, clathrin and lysosomal marker, LAMP1. A,B) Localization of clathrin in the apical pole of the epithelium 10 and 30 min after lysozyme injection, respectively. C) Noticeable decreased fluorescence of labeled clathrin in non-injected frogs. D-H) Double-labeling of lysozyme (green) and clathrin (red) demonstrating their colocalization (yellow) 10 min after lysozyme treatment (D-F) and following divergence of both fluorescence signals within 30 min (G, H, arrows). I, J) Double-labeling of lysozyme (green) and LAMP1 (red) 10 and 30 min after protein injection; note the absence of lysozyme and LAMP1 colocalization within 30 min of the experiment. Scale bars, 25 μm.

revealed that megalin and cubilin were clearly expressed in the kidney of lysozyme-injected frogs in contrast with immuno-negative control animals. Labeling for both receptors was found in the apical area of the proximal tubule cells (Figure 1 G-K). The internalization of some macromolecules in the *Xenopus pronephros*[2] and larval zebrafish[21] involving both megalin and cubilin has been shown. In our recent work, the expression of endocytic receptors associated with the tubular absorption of YFP was demonstrated in the mesonephros of *R. temporaria*.[12] According to the present results, the expression of megalin was more intensive than one of cubilin that corresponds with the similar data about the general lower level of cubilin expression in zebrafish pronephric kidney.[21]

Immunohistochemistry demonstrated time-dependent internalization of endocytic receptors similar to initial lysozyme internalization. Anti-lysozyme staining closely coincided with the sites of megalin and cubilin localization revealed in the tubular cells (Figure 1), suggesting that the uptake of lysozyme was accompanied by the expression of endocytic receptors. These results are in good agreement with our previous data, which has been demonstrated that 15 and 30 min after introduction YFP was colocalized with megalin and cubilin in vesicular structures in frog tubular epithelium.[12] However, the identity of the intracellular vesicular compartments containing YFP and endocytic receptors has been remained unclear. Immuno-electron microscopy confirmed the primary localization of both receptors in apical endocytic structures of the epitheliocytes including intermicrovillar pits, apical vesicles and dense apical tubules (Figure 2 F,G). This corresponds to the data about intracellular distribution of endocytic receptors in the mammalian metanephros and in the Xenopus pronephros.[2,16] In the proximal tubules, megalin and cubilin can be localized to the brush border, coated pits, endocytic vesicles, dense apical tubules and in small and large endosomes.[16,35,36] Based on our results, the expression of endocytic receptors in the proximal tubules of *R. temporaria* was appeared to be induced by the entering of filtered lysozyme into the tubular lumen. The undetectable expression of megalin and cubilin in the control animals (PBS-injected or non-injected) may be explained by the low metabolic activity in wintering frogs. The series of investigations in amphibians - *Hyla arborea*,[37] *R. pipiens*[38] and *R. esculenta*[14] - directed at the study of the mechanisms of biochemical and morphological adaptation to seasonal and environmental variations revealed the noticeable decrease of endocytic activity in the renal proximal tubules. The ultrastructural changes of the proximal tubule cells were connected with reduction of the number of apical vesicles and dense tubules, as well as mitochondria and endoplasmic reticulum. The decline of the activity of some enzymes, linked to membrane transport and energetic metabolism also demonstrated a sign of decreased endocytosis during hibernation.[14]

To identify the early step of lysozyme internalization in the frog tubule cells we used dual labeling employing markers of clathrin-dependent and caveolin-dependent endocytosis. The increased expression of clathrin in the proximal tubules after lysozyme injection was detected (Figure 3 A-C). Immunocytochemical analysis confirmed the typical intracellular distribution of clathrin in the epithelial cells (Figure 2E) reflecting the formation of coated pits and vesicles.[39,40] The availability of clathrin in the tubular cells in control frogs (without lysozyme injection) confirms the data about constitutive expression of clathrin and its involving in the continuous uptake of essential nutrients in mammalian cells.[41] It is also established that clathrin coats can spontaneously assemble at the apical membrane.[42] On the contrary, the negative staining with caveolin antibodies demonstrates the absence of alternative pathway of lysozyme endocytosis in the frog tubular cells described in some cell types of mammals.[43] The initial lysozyme and clathrin colocalization in the same apical cell structures (10 min after injection) indicates that lysozyme was internalized *via* clathrin-coated vesicles. The further disappearance of lysozyme and clathrin overlapping (20 and 30 min after injection) may be a result of the removal of protein to the endosomal compartment, possibly early endosomes. Megalin and cubilin are known to be internalized by clathrin-coated invaginations on the plasma membrane that eventually detached to form clathrin-coated vesicles, then delivered to endosomes and recycled to the apical membrane.[16,35] In consideration of these data and our results about clathrin and lysozyme colocalization and megalin and cubilin expression we conclude that lysozyme is absorbed by receptor-mediated clathrin-depending pathway in the frog proximal tubule cells.

The increased number of lysozyme-absorbing tubules on kidney sections as the number and size of lysozyme-containing vesicles in the tubule cells 30 min after injection reflect the pronounced accumulation of protein (Figure 1 A-C). However, the localization of these vesicles remained mainly apical without extending to the more basal area of the cytoplasm. Double immunocytochemical labeling with anti-lysozyme and LAMP1 antibodies did not reveal the overlap within 30 min of experiment. It indicates that lysozyme is retained within endosomal compartment during this time. This result is not conformed to the data about lysosomal accumulation and time-depending degradation of lysozyme and other protein in the mammalian kidney. It was shown that lysozyme reached lysosomes within 10-15 min after injection,[22,29] and maximum accumulation of radioactively labeled lysozyme in the lysosomal fraction was observed after 30 min.[25] The most results in mammals demonstrate that intracellular trafficking of various proteins from endocytic vesicles to lysosomes is rapid process and varies among some minutes.[22,24,44] Similar retention of lysozyme in the endosomal compartment was occurred under specific experimental conditions or by the some kidney disorders.[22,23] So, in maleate-treated rats, the decreased rate of fusion of numerous lysozyme-containing vacuoles with lysosomes and the essential reduce of lysosomal digestion of lysozyme were noted.[22] Lysozyme accumulation in the endosomal compartment of the frog tubule cells may be connected with lower metabolic rate and following inhibition of the protein intracellular traffic in hibernating frogs that confirms well known energy dependence of the endocytic system. Our light and electron microscopy observations confirm the proximal tubule subdivision (early and late segments) in *R. temporaria* previously described in some amphibians.[13,14,15,37,45,46] These segments can be easily identified on the basis of morphological features including height and shape of the epithelial cells, length and density of microvilli, and nucleus location. The fluorescence pattern of lysozyme in the early proximal tubule was more intensive and pronounced than in the late segment (Figure 1 B,C). Similar results were also obtained for the distribution of clathrin and expression of megalin and cubilin. These findings are in a good agreement with data about the gradient of macromolecule uptake along the proximal tubules in the kidney of lower vertebrates.[1,47] Thus, we investigated the tubular absorption of lysozyme in the frog kidney after its intravenous injection using immunocytochemistry and immunohistochemistry with specific markers of endocytic pathways and some intracellular compartments. Confocal microscopy demonstrated time-dependent uptake of lysozyme accompanied by the expression of endocytic receptors, megalin and cubilin, and by the formation of clathrin vesicles. Following internalization *via* clathrin-coated vesicles, lysozyme is transferred to endosomes but did not reach lysosomes within 30 min after injection. This retaining of absorbed protein in the endosomal compartment may be connected with lower standard metabolic rate in hibernating frogs and respective reduction of the intracellular traffic of absorbates. To clarify this peculiarity of lysozyme accumulation, the time-course of

such experiment should be extended and comparative examination of protein uptake in the frog kidney in different physiological states should be carried out.

In the present work, we provided the evidence that lysozyme is filtered through the glomeruli and absorbed by receptor-mediated clathrin-dependent endocytosis in the proximal tubule cells of wintering frog *R. temporaria*. We conclude that in frog mesonephros the process of protein reabsorption is mediated by megalin and cubilin that confirms the critical role of endocytic receptors in the renal protein uptake in amphibians as in mammals. The data obtained allow using the mesonephros of anuran amphibians as a convenient and perspective model for further *in vivo* investigation of the mechanisms of endocytosis and its regulation under different physiological and environmental conditions.

References

1. Zhou X, Vize PD. Proximo-distal specialization of epithelial transport processes within the Xenopus pronephric kidney tubules. Develop Biol 2004;271:322-38.
2. Christensen E, Raciti D, Reggiani L, Verroust PJ, Brändli AW. Gene expression analysis defines the proximal tubule as the compartment for endocytic receptor-mediated uptake in the Xenopus pronephric kidney. Pflügers Arch 2008;456: 1163-76.
3. Tanner GA, Rippe C, Shao Y, Evan AP, Williams JC Jr. Glomerular permeability to macromolecules in the Necturus kidney. Am J Physiol Renal Physiol. 2009;296: F1269-78.
4. Kumano T, Konno N, Wakasugi T, Matsuda K, Yoshizawa H, Uchiyama M. Cellular localization of a putative Na(+)/H(+) exchanger 3 during ontogeny in the pronephros and mesonephros of the Japanese black salamander (Hynobius nigrescens Stejneger). Cell Tissue Res 2008;331:675-85.
5. Gross ML, Hanke W, Koch A, Ziebart H, Amann K, Ritz E. Intraperitoneal protein injection in the axolotl: the amphibian kidney as a novel model to study tubulointerstitial activation. Kidney Int 2002;62:51-9.
6. Gross ML, Piecha G, Bierhaus A, Hanke W, Henle T, Schirmacher P, et al. Glycated and carbamylated albumin are more "nephrotoxic" than unmodified albumin in the amphibian kidney. Am J Physiol Renal Physiol 2011;301:F476-85.
7. Van Timmeren MM, Gross ML, Hanke W, Klok PA, van Goor H, Stegeman CA, et al. Oleic acid loading does not add to the nephrotoxic effect of albumin in an amphibian and chronic rat model of kidney injury. Nephrol Dial Transplant 2008;23:3814-23.
8. Christensen EI, Nielsen R, Birn H. From bowel to kidneys: the role of cubilin in physiology and disease. Nephrol Dial Transplant 2013;28:274-81.
9. Seliverstova EV, Burmakin MV, Natochin YuV. Renal clearance of absorbed intact GFP in the frog and rat intestine. Comp Biochem Physiol A Mol Integr Physiol 2007; 147:1067-73.
10. Prutskova NP. Renal filtration and reabsorption of GFP in Rana temporaria: effect of arginine-vasotocin. J Evol Biochem Physiol 2011;47:59-68.
11. Prutskova NP, Seliverstova EV. Tubular GFP uptake pattern in the rat and frog kidneys. Comp Biochem Physiol A Mol Integr Physiol 2011;160:175-83.
12. Prutskova NP, Seliverstova EV. Absorption capacity of renal proximal tubular cells studied by combined injections of YFP and GFP in Rana temporaria L. Comp Biochem Physiol A Mol Integr Physiol 2013;166:138-46.
13. Uchiyama M, Murakami T, Yoshizawa H, Wakasugi C. Structure of the kidney in the crab-eating frog, Rana cancrivora. J Morphol 1990;204:147-56.
14. Fenoglio C, Vaccarone R, Chiari P, Gervaso MV. An ultrastructural and cytochemical study of the mesonephros of Rana esculenta during activity and hibernation. Eur J Morphol 1996;34:107-21.
15. Møbjerg N, Jespersen A, Wilkinson M. Morphology of the kidney in the West African caecilian, Geotrypetes seraphini (Amphibia, Gymnophiona, Caeciliidae). J Morphol 2004;262:583-607.
16. Christensen EI, Birn H. Megalin and cubilin: synergistic endocytic receptors in renal proximal tubule. Am J Physiol Renal Physiol 2001;280:F562-73.
17. Christensen EI, Verroust PJ, Nielsen R. Receptor-mediated endocytosis in renal proximal tubule. Pflügers Arch 2009;458: 1039-48.
18 Amsellem S, Gburek J, Hamard G, Nielsen R, Willnow TE, Devuyst O, et al. Cubilin is essential for albumin reabsorption in the renal proximal tubule. J Am Soc Nephrol 2010;21:1859-67.
19. Fyfe JC, Madsen M, Højrup P, Christensen EI, Tanner SM, de la Chapelle A, et al. The functional cobalamin (vitamin B12)-intrinsic factor receptor is a novel complex of cubilin and amnionless. Blood 2004;103:1573-9.
20. Coudroy G, Gburek J, Kozyraki R, Madsen M, Trugnan G, Moestrup SK, et al. Contribution of cubilin and amnionless to processing and membrane targeting of cubilin-amnionless complex. J Am Soc Nephrol 2005;16:2330-7.
21. Anzenberger U, Bit-Avragim N, Rohr S, Rudolph F, Dehmel B, Willnow TE, et al. Elucidation of megalin/LRP2-dependent endocytic transport processes in the larval zebrafish pronephros. J Cell Sci 2006;119: 2127-37.
22. Christensen EI, Maunsbach AB. Proteinuria induced by sodium maleate in rats: effects on ultrastructure and protein handling in renal proximal tubule. Kidney Int 1980;17:771-87.
23. Maack T, Johnson V, Kau ST, Figueiredo J, Sigulem D. Renal filtration, transport, and metabolism of low-molecular-weight proteins: a review. Kidney Int 1979;16:251-70.
24. Nielsen S. Time course and kinetics of proximal tubular processing of insulin. Am J Physiol 1992;262:F813-22.
25. Ottosen PD, Bode F, Madsen KM, Maunsbach AB. Renal handling of lysozyme in the rat. Kidney Int 1979;15: 246-54.
26. Sumpio BE, Maack T. Kinetics, competition, and selectivity of tubular absorption of proteins. Am J Physiol 1982;243:F379-92.
27. Franssen EJ, van Amsterdam RG, Visser J, Moolenaar F, de Zeeuw D, Meijer DK. Low molecular weight proteins as carriers for renal drug targeting: naproxen-lysozyme. Pharm Res 1991;8:1223-30.
28. Prakash J, van Loenen-Weemaes AM, Haas M, Proost JH, Meijer DK, Moolenaar F, et al. Renal-selective delivery and angiotensin-converting enzyme inhibition by subcutaneously administered captopril-lysozyme. Drug Metab Dispos 2005;33:683-8.
29. Cojocel C, Maita K, Baumann K, Hook JB. Renal processing of low molecular weight proteins. Pflugers Arch 1984;401:333-9.
30. Leheste JR, Rolinski B, Vorum H, Hilpert J, Nykjaer A, Jacobsen C, et al. Megalin knockout mice as an animal model of low molecular weight proteinuria. Am J Pathol 1999;155:1361-70.
31. Hysing J, Tolleshaug H, Curthoys NP. Reabsorption and intracellular transport of cytochrome c and lysozyme in rat kidney. Acta Physiol Scand 1990;140:419-27.
32. Zheng F, Cai W, Mitsuhashi T, Vlassara H. Lysozyme enhances renal excretion of advanced glycation endproducts in vivo and suppresses adverse age-mediated cellular effects in vitro: a potential AGE sequestration therapy for diabetic nephropathy? Mol Med 2001;7:737-47.
33. Weyer K, Stormm T, Shan J, Vainio S, Kozyraki R, Verroust PJ, et al. Mouse model of proximal tubule endocytic dysfunction. Nephrol Dial Transplant 2011;26: 3446-51.

34. Kozyraki R, Fyfe J, Verroust PJ, Jacobsen C, Dautry-Varsat A, Gburek J, et al. Megalin-dependent cubilin-mediated endocytosis is a major pathway for the apical uptake of transferrin in polarized epithelia. Proc Natl Acad Sci USA 2001;98: 12491-6.
35. Biemesderfer D, Dekan G, Aronson PS, Farquhar MG. Assembly of distinctive coated pit and microvillar microdomains in the renal brush border. Am J Physiol 1992;262: F55-67.
36. Seetharam B, Christensen EI, Moestrup SK, Hammond TG, Verroust PJ. Identification of rat yolk sac target protein of teratogenic antibodies, gp280, as intrinsic factor-cobalamin receptor. J Clin Invest 1997;99:2317-22.
37. Pons G, Guardabassi A, Pattono P. The kidney of Hyla arborea (L.) (amphibia hulidae) in autumn, winter and spring: histological and ultrastructural observations. Ital J Zool 1982;16:261-81.
38. Karnovsky MJ, Himmelhoch SR. Seasonal and starvation-induced changes in enzymatic pattern of frog nephron. Am J Physiol 1961;201:781-5.
39. Rodman JS, Kerjaschki D, Merisko E, Farquhar MG. Presence of an extensive clathrin coat on the apical plasmalemma of the rat kidney proximal tubule cell. J Cell Biol. 1984;98:1630-36.
40. Traebert M, Roth J, Biber J, Murer H, Kaissling B. Internalization of proximal tubular type II Na-P(i) cotransporter by PTH: immunogold electron microscopy. Am J Physiol Renal Physiol 2000;278:F148-54.
41. Brodsky FM, Chen CY, Knuehl C, Towler MC, Wakeham DE. Biological basket weaving: formation and function of clathrin-coated vesicles. Annu Rev Cell Dev Biol 2001;7:517-68.
42. Ehrlich M, Boll W, Van Oijen A, Hariharan R, Chandran K, Nibert ML, et al. Endocytosis by random initiation and stabilization of clathrin-coated pits. Cell 2004;118:591-605.
43. Brown D, Stow JL. Protein trafficking and polarity in kidney epithelium: from cell biology to physiology. Physiol Rev 1996;76: 245-97.
44. Park CH. Time course and vectorial nature of albumin metabolism in isolated perfused rabbit PCT. Am J Physiol 1988;255 :F520-8.
45. Clothier RH, Worley RT, Balls M. The structure and ultrastructure of the renal tubule of the urodele amphibian, Amphiuma means. J Anat 1978;127:491-504.
46. Forster J, Steels PS, Boulpaep EL. Organic substrate effects on and heterogeneity of Necturus proximal tubule function. Kidney Int 1980;17:479-90.
47. Youson JH. Absorption and transport of ferritin and exogenous horseradish peroxidase in the opisthonephric kidney of the sea lamprey II. The tubular nephron. Cell Tissue Res 1975;157:503-16.